3D Aneurysm Wall Enhancement is Associated with Symptomatic Presentation

Ashrita Raghuram, BSE[1], **Sebastian Sanchez, MD**[1], **Linder Wendt, MS**[4], **Steven Cochran, BS**[5], **Daizo Ishii, MD**[2], **Carlos Osorno-Cruz, BS**[2], **Girish Bathla, MD**[3], **Tim Koscik, PhD**[5], **James Torner, PhD**[2,4], **David Hasan, MD MSc**[6], **Edgar A Samaniego, MD,MS**[1,2,3]

[1.]Department of Neurology, The University of Iowa Hospitals and Clinics, Iowa City, IA

[2.]Department of Neurosurgery, The University of Iowa Hospitals and Clinics, Iowa City, IA

[3.]Department of Radiology, The University of Iowa Hospitals and Clinics, Iowa City, IA

[4.]Institute for Clinical and Translational Science, The University of Iowa, Iowa City, IA

[5.]Department of Psychiatry, The University of Iowa Hospitals and Clinics, Iowa City, IA

[6.]Department of Neurosurgery, Duke University, Durham, NC

Abstract

Background: Aneurysm wall enhancement (AWE) is a potential surrogate biomarker for aneurysm instability. Previous studies have assessed AWE using 2D multiplanar methods, most of which were conducted qualitatively. A new quantitative tool to map 3D-AWE was studied on a large cohort of patients.

Methods: Saccular aneurysms were imaged prospectively with 3T high resolution magnetic resonance imaging (HR-MRI). 3D-AWE maps of symptomatic (defined as ruptured or presentation with sentinel headache/cranial nerve neuropathy) and asymptomatic aneurysms were created by extending orthogonal probes were extended from aneurysm segmentations into the wall. Three metrics were used to characterize enhancement: 3D circumferential AWE (3D-CAWE), aneurysm-specific contrast uptake (SAWE), and focal AWE (FAWE). Aneurysms with a circumferential AWE higher than the corpus callosum (3D-CAWE $\geq$ 1) were classified as 3D-CAWE+. Symptomatic presentation was predicted with univariate and multivariate logistic models. Aneurysm size, size ratio, aspect ratio, irregular morphology, and PHASES and ELAPSS scores were compared with the new AWE metrics. Bleb and microhemorrhage analyses were also performed.

Results: Ninety-three aneurysms were analyzed. 3D-CAWE, SAWE, and FAWE were associated with symptomatic status (OR=1.34,1.25, and 1.08 respectively). A multivariate model including aneurysm size, 3D-CAWE+, age, female sex, and FAWE detected symptomatic status with 80% specificity and 90% sensitivity (AUC=0.914, NPV=0.967). FAWE was also associated with irregular morphology and high-risk location (*p*=0.043, *p*=0.001 respectively). In general,

CORRESPONDING AUTHOR: Edgar A Samaniego MD, MS, Associate Professor of Neurology, Neurosurgery, and Radiology, 200 Hawkins Drive, Iowa City, Iowa 52246, United States of America, edgarsama@gmail.com, 319-333-4460.

COMPETING INTERESTS: None

blebs enhanced 56% more than the aneurysm body. Areas of microhemorrhage colocalized with increased SAWE (p=0.047).

Conclusions: 3D-AWE mapping provides a new set of metrics that could potentially improve the identification of symptomatic aneurysms.

Keywords

Aneurysm; Wall Enhancement; Symptomatic; 3D Mapping

INTRODUCTION:

Aneurysm wall enhancement (AWE) based on high resolution magnetic resonance imaging (HR-MRI) could potentially identify brain aneurysms at risk of growth or rupture.(1, 2) Histopathological studies have shown that AWE is associated with increased proinflammatory markers and might identify areas of increased vasa vasorum, neovascularization, and macrophage infiltration.(3-5) AWE has also been consistently described in growing, symptomatic, and ruptured aneurysms.(2, 6, 7) These findings highly suggest that AWE might be a surrogate biomarker of aneurysm instability.

AWE has been previously characterized by different methods. Circumferential AWE (CAWE) has been associated with aneurysm growth or rupture in qualitative and quantitative studies. (8, 9) Focal AWE (FAWE) has been colocalized to areas of aneurysm rupture or prone to rupture.(10, 11) These assessments of AWE have been performed on 2D multiplanar imaging and generally involved manual selection of regions of interest (ROIs). This approach limits analysis of the entire aneurysm, which might hinder determining the risk of rupture. We have developed a new semiautomated pipeline for measuring AWE in three dimensions (3D-AWE).(12) The aim of this study was to analyze a large cohort of saccular aneurysms with 3D-AWE maps. The accuracy of AWE metrics generated through this method was tested in symptomatic and incidentally found, asymptomatic aneurysms.

METHODS:

Image Acquisition and Processing:

Aneurysms were prospectively imaged with HR-MRI between May 2018 and November 2021 after approval from the University of Iowa institutional review board. Saccular aneurysms larger than 2 mm in size were included. Fusiform, thrombosed, or small (<2 mm) aneurysms were excluded. MRIs were performed on a 3T MRI (MAGNETOM Skyra, Siemens); T1-weighted (T1), T1+gadolinium (T1+Gd), quantitative susceptibility mapping (QSM), and time of flight (TOF) sequences were obtained. Specific imaging parameters are described in Supplementary Table S1. T1 and T1+Gd images were isotropically resampled, denoised, and registered.(12) The range of raw signal intensity (SI) values did not change after processing.

3D Reconstruction and Surface Mapping:

A post-acquisition pipeline developed for 7T-MRI was adapted to 3T-MRI. The goal of this semiautomated method was to generate 3D-AWE maps of the entire aneurysm.(12)

Manual segmentations of the aneurysm sac and parent vessel were created using T1 images. Segmentations were carefully created and verified to allow accurate probing of the aneurysm wall while avoiding oversampling of surrounding structures. Using custom MATLAB R2021b (MathWorks, Natick, MA) scripts, SI probes were orthogonally extended from the aneurysm lumen 0.5 mm into the aneurysm wall.(13) The number of probes created was proportional to the surface area of the aneurysm. The maximal SI value and spatial location of each probe were used to create 3D surface maps, histograms, and survival plots representing the distribution of SI along the entire aneurysm wall for T1 and T1+Gd images. (Figure 1). SI values were normalized to the genu of the corpus callosum (CC).

A separate analysis of enhancement in aneurysm blebs was conducted. Aneurysm blebs, identified as thin outpouchings of the aneurysm wall, were isolated from the aneurysm body, and their SI was compared to the rest of the aneurysm body.(14)

Quality Control:

Sampling of structures beyond the aneurysm wall, such as cerebrospinal fluid, bone, or surrounding brain tissue (Supplementary Figure S1) was identified by histogram analysis and verified on 3D heatmaps. This artifact was removed by excluding probes with values lower than the 70th percentile of the SI label. Final 3D-AWE reconstructions were visually examined for accuracy, after comparison with source images.

Definitions of Aneurysm Wall Enhancement Metrics:

Three metrics were used to describe circumferential, dynamic, and focal patterns of AWE. Previous 2D methods used circumferential AWE (CAWE) to quantify enhancement along the circumference of the wall within one plane.(8, 9) 3D-CAWE samples the entire aneurysm, and is defined by the mean SI of all probes in T1+Gd images. Because SI values were originally normalized to the CC, aneurysms that enhanced (on average) more than the CC (3D-CAWE $\geq$ 1) were defined as 3D-CAWE+. Aneurysms less enhancing than the CC were therefore classified as 3D-CAWE−. The dynamic uptake of contrast by the aneurysm wall or the change in SI between T1 and T1+Gd has been previously described in 2D as the wall enhancement index (WEI)(9). The 3D equivalent is defined as specific AWE (SAWE), or the difference in mean SI between T1 and T1+Gd. Finally, the presence of FAWE is defined by areas of the aneurysm with increased AWE on 3D-AWE maps. Increased FAWE leads to a positive (right) skewness on histogram analysis.

Classification of Symptomatic Aneurysms:

Aneurysms were classified as symptomatic or asymptomatic. Symptomatic aneurysms included ruptured aneurysms, aneurysms accompanied with cranial nerve (CN) neuropathy due to pressure or inflammation, and aneurysms that presented with a sentinel headache (unusually severe and sudden within two weeks of presentation).(15, 16)

Comparison of 3D-AWE Pipeline to 2D-AWE:

To determine the correlation between the new 3D-AWE method with known objective methods of measuring AWE, we compared semiautomated measurements of 3D-AWE to manual 2D measurements in 68 aneurysms. 3D-CAWE normalized to the pituitary stalk

(CR_{stalk}) was compared to CR_{stalk} obtained by manual measurements, as described by Roa et al.(17) To evaluate the performance of the 3D-AWE pipeline with 2D-measurements, a sensitivity analysis was conducted in this subgroup of aneurysms to detect symptomatic status. Aneurysms were classified as enhancing or non-enhancing using the above definition of 3D-CAWE+ and the previously defined manual CR_{stalk} cutoff of 0.6.(17)

Morphological Characterization of Aneurysms:

Multiple comparisons were performed to determine the relationship between 3D-AWE and morphological metrics. Measurements of largest aneurysm diameter, neck width, sac height, and parent vessel diameter were manually conducted on either digital subtraction angiography (DSA), computed tomography angiography, or magnetic resonance angiography on the best available projection. Aneurysm size (the largest dimension), size ratio (SR = ratio of aneurysm sac height to average parent vessel diameter), and aspect ratio (AR = ratio of perpendicular sac height to neck width) were calculated for each aneurysm. (18) Irregular aneurysms were identified by two experienced investigators, according to definitions outlined by Hackenberg et al.(14) Disagreements were adjudicated by a third senior investigator. To evaluate growth or rupture risk using clinical predictive scales, ELAPSS and PHASES scores were calculated for each aneurysm.(19, 20) For dichotomous comparisons of enhancement, aneurysms were categorized as irregular or regular, size 7 or <7 mm, high risk location (anterior communicating artery complex (ACOM), posterior communicating artery (PCOM), and basilar artery) vs. lower risk locations, ELAPSS 15 or <15, PHASES 5 or <5, and symptomatic vs. asymptomatic. (19-22)

Microhemorrhage Analysis and Reconstruction:

Aneurysms fwith microhemorrhage based on QSM imaging were classified as QSM+. Using the MATLAB toolbox, STI Suite, Laplacian-based phase processing was performed on QSM images to produce tissue phase visualization.(23) The subsequent images were then co-registered on 3D-Slicer with TOF-MRA sequences. 3D volumetric reconstructions were conducted by incorporating the microhemorrhage segmentation with the aneurysm at an optimal susceptibility threshold of 0.1 ppm, according to Nakagawa et al.(24)

Statistical Analysis:

Statistical analysis was conducted using either IBM SPSS Statistics for Windows, Version 27.0 (IBM Corp, Armonk, NY) or R, Version 4.1.2 (R Core Team, Vienna, Austria). Categorical data are represented as frequency (percentage). Shapiro-Wilk tests were conducted on continuous data to determine whether they were normally distributed. Normally distributed variables are represented as mean ± SD. Non-normally distributed variables are represented as median (IQR). Comparisons between normally distributed data were conducted using Student's t-tests and Pearson correlations. Comparisons involving non-normally distributed data were conducted using Mann-Whitney U tests and Spearman's correlations. Comparisons between unpaired categorical data were conducted using Pearson's chi-squared test, or Fisher's exact test.

To assess the effect of various predictors on the likelihood that a given aneurysm would be symptomatic, a series of univariate logistic regression models were constructed, providing

odds ratios (OR), confidence intervals (CI), and *p* values. Using all variables analyzed in the univariate setting, a multivariable model was constructed using a forward stepwise selection approach oriented toward minimizing the Akaike Information Criterion (AIC) of the model. At each step of this selection procedure, candidate variables were assessed to see which one would most greatly reduce the AIC of the model. After this variable was added, the pool of candidate variables was reduced to no longer include the variable that was just added to the model or any variables that were correlated with that variable with a correlation of greater than 0.5 or less than −0.5. The predicted odds generated by the multivariate model were converted into probabilities that an aneurysm would be symptomatic for each of the aneurysms in our data. Sensitivity, specificity, and negative predictive value (NPV) measurements were also computed for all candidate predictor variables. Optimal cutoff points for continuous measures were found using Youden's J statistic.

RESULTS:

Demographics and Aneurysm Characteristics:

A total of 233 patients underwent HR-MRI. One hundred sixty patients with fusiform (n = 43), thrombosed (n = 10), small (<2 mm) aneurysms (n = 20), and poor quality/incomplete imaging (n = 87) were excluded. A total of 73 patients with 93 aneurysms (88 unruptured, 5 ruptured) were included. Of these aneurysms, 73 (78%) were treated upon presentation. Five (7%) aneurysms were surgically clipped and 68 (93%) were endovascularly treated. Demographic and morphological data are described in Supplementary Table S2 . Twenty (27%) aneurysms were classified as symptomatic and are described in Supplementary Table S3. A median (IQR) of 316 (421) SI probes were generated per aneurysm.

Comparison of 3D-AWE Pipeline to 2D AWE:

A subgroup of sixty-eight aneurysms were analyzed with both the semi-automated 3D-AWE method and the manual 2D CR_{stalk} method. Fiveteen (22%) aneurysms of this cohort were symptomatic. The 3D-AWE method had a strong correlation with manual 2D measurements of SI (Spearman's rho = 0.828) (Supplementary Figure S2). Using the manual method (CR_{stalk} 0.6), 11 (16%) aneurysms were classified as enhancing. Of these 11 aneurysms, only 2 (18%) were symptomatic (p=0.735). Eighteen (26%) aneurysms were classified as 3D-CAWE+ (3D-CAWE   1), and 8 (44%) were symptomatic (p=0.008). 3D-CAWE+ (53% sensitivity, 81% specificity, AUC = 0.67) outperformed CR_{stalk} (13% sensitivity, 83% specificity, AUC = 0.48) in detecting symptomatic aneurysms in this subgroup analysis.

Aneurysm Wall Enhancement in Symptomatic Aneurysms:

Age, aneurysm size, SR, AR, 3D-CAWE, SAWE, and FAWE (skewness) were independent predictors of symptomatic status. (Table, Supplementary Table S4).

In some aneurysms, the three enhancement metrics (3D-CAWE, SAWE, and FAWE) were useful in predicting symptomatic status regardless of aneurysm size (Figure 2). Multivariate models that were fixed to include 3D-CAWE, SAWE, or FAWE as predictors were highly sensitive and specific. (Supplementary Table S5). The best multivariate model, including age, size, 3D-CAWE+, skewness, and female covariates, had 80% specificity

and 90% sensitivity in detecting symptomatic aneurysms (AUC = 0.914, NPV = 0.967). (Supplementary Figure S3).

Using the best model, the predicted probability of symptomatic status was calculated for each aneurysm. Fourteen (15%) of the aneurysms in the cohort had a higher than 50% probability of symptomatic status. Most of these aneurysms (71%) actually presented as symptomatic aneurysms. Fifty-one (55%) aneurysms had <10% probability of being symptomatic, and only one (2%) of these aneurysms, an 8 mm M2 MCA aneurysm, was actually symptomatic at presentation. These aneurysms were smaller in size [median (IQR) = 4.6 (1.75) vs. 6.8 (4.6), $p < 0.001$], had a lower SR [median (IQR) = 2.17 (1.75) vs. 2.67 (2.26), $p = 0.02$], and a lower AR [median (IQR) = 1.35 (0.67) vs. 1.67 (1.51), $p = 0.03$]. These aneurysms were also less enhancing, with a lower 3D-CAWE [mean ± SD = 0.80 ± 0.24 vs. 0.97 ± 0.27, $p = 0.003$], lower SAWE [median (IQR) = 0.16 (0.20) vs. 0.31 (0.39), $p = 0.002$], and lower FAWE [mean ± SD = 0.32 ± 0.74 vs. 0.19 ± 0.57, $p < 0.001$]. These aneurysms were also less likely to be present in smokers ($p = 0.027$) and had lower ELAPSS scores (mean ± SD = 13 ± 6 vs. 16 ± 8, $p = 0.039$).

Thirty-one (33%) of all the aneurysms in the cohort had a greater than 20% predicted probability of symptomatic presentation. Of these 31 aneurysms, 9 (29%) were small (<7 mm) in size. Of these 9 small, high-risk aneurysms, 6 (66%) were 3D-CAWE+ and 7 had a positive skew (FAWE). Although they had low average PHASES (3.8) and ELAPSS (12.7) scores, these aneurysms were highly enhancing (mean± SD 3D-CAWE = 0.9±0.2 and FAWE/skew = 0.2±0.8).

AWE Metrics and Morphology:

Aneurysms   7 mm in diameter (n = 64) had a higher 3D-CAWE [mean ± SD = 0.99 ± 0.21 vs. 0.82 ± 0.28, $p = 0.004$] and higher SAWE [median(IQR) = 0.30 (0.26) vs. 0.16 (0.27), $p = 0.006$] than smaller aneurysms. Symptomatic aneurysms had a higher 3D-CAWE (mean ± SD = 1.03 ± 0.25) than asymptomatic aneurysms (mean ± SD = 0.83 ± 0.26, $p = 0.003$). Most symptomatic aneurysms were 3D-CAWE+ [13 symptomatic (65%) vs. 7 (35%) asymptomatic aneurysms ($p < 0.001$)].

FAWE was higher in aneurysms with irregular morphology (n = 34, mean ± SD = 0.11 ± 0.55 vs. −0.20 ± 0.78, $p = 0.043$), high PHASES (5) scores (n = 44, mean ± SD = 0.25 ± 0.52 vs. −0.39 ± 0.73, $p < 0.001$), high ELAPSS (15) scores (n = 44, mean ± SD = 0.10 ± 0.54 vs. −0.25 ± 0.81, $p = 0.018$), and in symptomatic aneurysms (n = 20, mean ± SD = 0.20 ± 0.56 vs. −0.16 ± 0.73, $p = 0.045$). Aneurysms in high-risk locations (n = 35) had a higher FAWE compared to aneurysms in other locations (mean ± SD = 0.22 ± 0.61 vs. −0.27 ± 0.72, $p = 0.001$). This finding was consistent for smaller aneurysms (<7 mm) as well (mean ± SD = 0.29 ± 0.69 vs. −0.39 ± 0.75, $p = 0.001$).

Bleb Analysis:

Thirty-four aneurysms had irregular morphology; 21 (62%) had blebs and 4 (12%) were multilobulated. Approximately 61% of blebs enhanced more than the rest of the aneurysm. On average, these enhancing blebs had 17% higher SI and 56% more contrast uptake than the aneurysm sac (Figure 3). In each of the four multilobulated aneurysms, one lobe showed

increased SI compared to the rest of the aneurysm. These lobes had 11% higher SI and 65% more contrast uptake than the rest of the aneurysm.

Microhemorrhage Analysis:

Only 46 unruptured aneurysms were analyzed with QSM due to image artifact. Six aneurysms were QSM+ and showed increased enhancement in all three metrics (3D-CAWE, SAWE, and FAWE). SAWE was significantly higher in QSM+ compared to QSM- aneurysms [median (IQR) = 0.30 (0.23) vs. 0.13 (0.23), p = 0.047].

DISCUSSION:

AWE has consistently been associated with aneurysm instability. However, previous studies have been limited by 2D sampling of the aneurysm wall in multiplanar views. In this study, we demonstrated that 3D-AWE had a strong association with symptomatic presentation. 3D-CAWE, SAWE, and FAWE had a strong association with known features of aneurysm instability. 3D mapping of AWE may be a powerful method of identifying both symptomatic and highly unstable asymptomatic aneurysms.

Advantages of 3D-AWE Mapping

The analysis of AWE has been done both subjectively and objectively using 2D multiplanar imaging.(8, 17) Finding objective methods to measure AWE of the entire aneurysm in 3D may enhance our understanding of the possible association between AWE and the risk of aneurysm rupture. Khan et al. performed the first 3D mapping of MRI signal intensities of 25 aneurysms, but thresholding for enhancement was subjectively dichotomized, rather than using quantitative AWE metrics.(25) Veeturi et al. tested a pipeline for AWE visualization in 41 aneurysms, and the optimal normalization threshold was calibrated subjectively. This was a good first step of visualizing AWE of the entire aneurysm. However, the agreement between the enhancement areas defined by neuroradiologists and those obtained through their method was modest.(26)

The pipeline implemented in this analysis generates three strong AWE metrics that describe different biological processes. The first is 3D-CAWE, which is used to quantify AWE for the entire aneurysm relative to the corpus callosum based only on T1+Gd imaging. The second is SAWE, which compares the SI in T1 vs. T1+Gd images to determine the average level of contrast uptake for the entire aneurysm. And the third metric, FAWE, quantifies focal AWE, or regions of the aneurysm that are more enhancing than the rest of the aneurysm sac. This is measured using the skewness of the histogram on T1+Gd imaging. On top of having 3D color maps, the pipeline allows the generation of histograms that improve quality control and quantifies the distribution of enhancement along the aneurysm wall.

Aneurysm Wall Enhancement in Symptomatic Aneurysms

In a systematic review and meta-analysis of >1000 aneurysms, Molenberg et al. demonstrated a positive association between AWE and aneurysm rupture, growth, or symptomatic presentation.(27) A recent analysis of 341 aneurysms by Fu et al. identified AWE as an independent risk factor associated with symptomatic aneurysms (defined

by the presence of sentinel headache or oculomotor nerve palsy). Their study used 2D multiplanar qualitative and quantitative assessments of AWE.(7) Other studies have found a similar relationship between AWE and symptomatic presentation.(28) Our findings support the hypothesis that AWE can provide insight into potential aneurysm instability. The multivariate model generated through our pipeline used AWE, age, aneurysm size, and female sex in detecting symptomatic aneurysms with a 80% specificity and 90% sensitivity (AUC = 0.914, NPV = 0.967). Other known factors associated with higher risk of aneurysm rupture, such as SR, AR, location, size and high PHASES and ELAPSS scores, also had a strong correlation with every AWE metric generated through this pipeline.

FAWE and Bleb Analysis

Irregular morphology/the presence of blebs is a risk factor of aneurysm rupture.(29) In our analysis, aneurysms with irregular morphology had increased FAWE ($p = 0.043$). Small aneurysms in locations associated with a high risk of rupture also had increased FAWE ($p = 0.001$). Better methods are required to identify small aneurysms that would not conventionally be deemed as high a risk, based on ISUIA criteria. Smaller aneurysms (<7 mm), such as aneurysms located in ACOM, PCOM, and PICA, often present ruptured. In our cohort, these aneurysms had larger areas of FAWE when compared to larger aneurysms (Figure 2). 2D multiplanar studies have described the colocalization of FAWE with points of rupture.(10, 11) 3D-AWE mapping provides both quantitative and qualitative measures of such areas and might improve identification of these high-risk areas. On average, blebs took up 56% more contrast than the aneurysm sacs. (Figure 3). Compartmental analysis of contrast uptake might allow for identifying focal areas of wall thinning and/or degradation such as blebs or areas prone to develop blebs.

Microhemorrhage Analysis

In our cohort, 46 aneurysms had appropriate QSM imaging for analysis. Six QSM+ aneurysms had significantly higher SAWE ($p = 0.047$). Areas of microhemorrhage colocalized with increased AWE. This highlights the potential of using SAWE as a metric for identifying areas with a high risk of rupture. Qi et al. described a similar pharmacokinetic phenomenon in high-risk aneurysms with increased Gd uptake.(30) Since SAWE determines Gd uptake by comparing the difference between T1+Gd and T1, it could be used to identify aneurysms with high-risk areas associated with microhemorrhages.

Limitations:

Although this is the largest cohort of aneurysms analyzed with 3D-AWE mapping, it is skewed toward small and asymptomatic aneurysms. The size of our sample was limited by the quality of HR-MRI images, with motion artifact being the most common issue. To address this, we have shortened our protocol to decrease movement and improve patient compliance. Our 3D-AWE protocol models the aneurysm wall assuming a uniform wall thickness of 0.5 mm. For thicker-walled aneurysms (>0.5 mm) our measurements might not capture the entire wall and therefore might result in undersampling. For thin-walled aneurysms, oversampling can be accounted for using our quality control mechanisms (histogram analysis/CSF removal). Because segmentations of the aneurysm sac were created manually, a higher level of quality control was required. Another limitation of this pipeline

is the processing time due to the manual nature of segmentations. In total, the time for processing was about one hour per aneurysm, depending on size. Automating segmentation would further improve the efficiency of this pipeline. In addition, image artifacts from 3T MRI, such as cerebrospinal fluid contamination and luminal contamination posed a challenge for automation. We have created a robust method to address these artifacts.

CONCLUSIONS:

3D-AWE mapping has the potential to identify symptomatic aneurysms through a new set of AWE metrics. This new pipeline provides unique insights into the multifactorial process of aneurysm instability.

Supplementary Material

Refer to Web version on PubMed Central for supplementary material.

ACKNOWLEDGEMENTS:

ABBREVIATIONS:

HR-MRI	High-Resolution MRI
AWE	Aneurysm Wall Enhancement
T1+Gd	Post gadolinium contrast T1 weighted image
QSM	Quantitative susceptibility mapping
SI	Signal Intensity
3D-CAWE	Three-dimensional Circumferential Aneurysm Wall Enhancement
CAWE	Circumferential Aneurysm Wall Enhancement
SAWE	Specific Aneurysm Wall Enhancement
FAWE	Focal Aneurysm Wall Enhancement
IA	Intracranial Aneurysm
CC	Corpus Callosum
OR	Odds Ratio

| AUC	Area under curve
NPV	Negative predictive value

REFERENCES:

1. Gariel F, Ben Hassen W, Boulouis G, et al. Increased Wall Enhancement During Follow-Up as a Predictor of Subsequent Aneurysmal Growth. Stroke. 2020;51(6):1868–72. [PubMed: 32397927]

2. Vergouwen MDI, Backes D, van der Schaaf IC, et al. Gadolinium Enhancement of the Aneurysm Wall in Unruptured Intracranial Aneurysms Is Associated with an Increased Risk of Aneurysm Instability: A Follow-Up Study. AJNR Am J Neuroradiol. 2019;40(7):1112–6. [PubMed: 31221634]

3. Larsen N, von der Brelie C, Trick D, et al. Vessel Wall Enhancement in Unruptured Intracranial Aneurysms: An Indicator for Higher Risk of Rupture? High-Resolution MR Imaging and Correlated Histologic Findings. AJNR Am J Neuroradiol. 2018;39(9):1617–21. [PubMed: 30026386]

4. Zhong W, Su W, Li T, et al. Aneurysm Wall Enhancement in Unruptured Intracranial Aneurysms: A Histopathological Evaluation. J Am Heart Assoc. 2021;10(2):e018633. [PubMed: 33410330]

5. Shimonaga K, Matsushige T, Ishii D, et al. Clinicopathological Insights From Vessel Wall Imaging of Unruptured Intracranial Aneurysms. Stroke. 2018;49(10):2516–9. [PubMed: 30355091]

6. Wang X, Zhu C, Leng Y, et al. Intracranial Aneurysm Wall Enhancement Associated with Aneurysm Rupture: A Systematic Review and Meta-analysis. Acad Radiol. 2019;26(5):664–73. [PubMed: 29908979]

7. Fu Q, Wang Y, Zhang Y, et al. Qualitative and Quantitative Wall Enhancement on Magnetic Resonance Imaging Is Associated With Symptoms of Unruptured Intracranial Aneurysms. Stroke. 2021;52(1):213–22. [PubMed: 33349014]

8. Edjlali M, Guedon A, Ben Hassen W, et al. Circumferential Thick Enhancement at Vessel Wall MRI Has High Specificity for Intracranial Aneurysm Instability. Radiology. 2018;289(1):181–7. [PubMed: 29969070]

9. Omodaka S, Endo H, Niizuma K, et al. Circumferential wall enhancement in evolving intracranial aneurysms on magnetic resonance vessel wall imaging. J Neurosurg. 2018:1–7.

10. Matsushige T, Shimonaga K, Mizoue T, et al. Focal Aneurysm Wall Enhancement on Magnetic Resonance Imaging Indicates Intraluminal Thrombus and the Rupture Point. World Neurosurg. 2019;127:e578–e84. [PubMed: 30928597]

11. Larsen N, Fluh C, Saalfeld S, et al. Multimodal validation of focal enhancement in intracranial aneurysms as a surrogate marker for aneurysm instability. Neuroradiology. 2020;62(12):1627–35. [PubMed: 32681192]

12. Raghuram A, Varon A, Roa JA, et al. Semiautomated 3D mapping of aneurysmal wall enhancement with 7T-MRI. Sci Rep. 2021;11(1):18344. [PubMed: 34526579]

13. Harteveld AA, Denswil NP, Van Hecke W, et al. Data on vessel wall thickness measurements of intracranial arteries derived from human circle of Willis specimens. Data Brief. 2018;19:6–12. [PubMed: 29892609]

14. Hackenberg KAM, Algra A, Al-Shahi Salman R, et al. Definition and Prioritization of Data Elements for Cohort Studies and Clinical Trials on Patients with Unruptured Intracranial Aneurysms: Proposal of a Multidisciplinary Research Group. Neurocrit Care. 2019;30(Suppl 1):87–101. [PubMed: 31102238]

15. Linn FH, Wijdicks EF, van der Graaf Y, et al. Prospective study of sentinel headache in aneurysmal subarachnoid haemorrhage. Lancet. 1994;344(8922):590–3. [PubMed: 7914965]

16. Okawara SH. Warning signs prior to rupture of an intracranial aneurysm. J Neurosurg. 1973;38(5):575–80. [PubMed: 4711629]

17. Roa JA, Zanaty M, Osorno-Cruz C, et al. Objective quantification of contrast enhancement of unruptured intracranial aneurysms: a high-resolution vessel wall imaging validation study. J Neurosurg. 2020;134(3):862–9. [PubMed: 32032948]

18. Dhar S, Tremmel M, Mocco J, et al. Morphology parameters for intracranial aneurysm rupture risk assessment. Neurosurgery. 2008;63(2):185–96; discussion 96-7. [PubMed: 18797347]

19. Backes D, Rinkel GJE, Greving JP, et al. ELAPSS score for prediction of risk of growth of unruptured intracranial aneurysms. Neurology. 2017;88(17):1600–6. [PubMed: 28363976]

20. Greving JP, Wermer MJ, Brown RD, Jr., et al. Development of the PHASES score for prediction of risk of rupture of intracranial aneurysms: a pooled analysis of six prospective cohort studies. Lancet Neurol. 2014;13(1):59–66. [PubMed: 24290159]

21. Wiebers DO, Whisnant JP, Huston J 3rd, et al. Unruptured intracranial aneurysms: natural history, clinical outcome, and risks of surgical and endovascular treatment. Lancet. 2003;362(9378):103–10. [PubMed: 12867109]

22. Waqas M, Chin F, Rajabzadeh-Oghaz H, et al. Size of ruptured intracranial aneurysms: a systematic review and meta-analysis. Acta Neurochir (Wien). 2020;162(6):1353–62. [PubMed: 32215742]

23. Li W, Avram AV, Wu B, et al. Integrated Laplacian-based phase unwrapping and background phase removal for quantitative susceptibility mapping. NMR Biomed. 2014;27(2):219–27. [PubMed: 24357120]

24. Nakagawa D, Kudo K, Awe O, et al. Detection of microbleeds associated with sentinel headache using MRI quantitative susceptibility mapping: pilot study. J Neurosurg. 2018:1–7.

25. Khan MO, Toro Arana V, Rubbert C, et al. Association between aneurysm hemodynamics and wall enhancement on 3D vessel wall MRI. J Neurosurg. 2020:1–11.

26. Veeturi SS, Pinter NK, Monteiro A, et al. An Image-Based Workflow for Objective Vessel Wall Enhancement Quantification in Intracranial Aneurysms. Diagnostics (Basel). 2021;11(10).

27. Molenberg R, Aalbers MW, Appelman APA, et al. Intracranial aneurysm wall enhancement as an indicator of instability: a systematic review and meta-analysis. Eur J Neurol. 2021;28(11):3837–48. [PubMed: 34424585]

28. Zhu C, Wang X, Eisenmenger L, et al. Wall enhancement on black-blood MRI is independently associated with symptomatic status of unruptured intracranial saccular aneurysm. Eur Radiol. 2020;30(12):6413–20. [PubMed: 32666320]

29. Salimi Ashkezari SF, Detmer FJ, Mut F, et al. Blebs in intracranial aneurysms: prevalence and general characteristics. J Neurointerv Surg. 2021;13(3):226–30. [PubMed: 32680877]

30. Qi H, Liu X, Liu P, et al. Complementary Roles of Dynamic Contrast-Enhanced MR Imaging and Postcontrast Vessel Wall Imaging in Detecting High-Risk Intracranial Aneurysms. AJNR Am J Neuroradiol. 2019;40(3):490–6. [PubMed: 30792252]

KEY MESSAGES:

Aneurysm wall enhancement (AWE) may predict symptomatic presentation, growth, or rupture. Most studies use multiplanar 2D methods to determine AWE. 3D-AWE metrics were strongly associated with symptomatic presentation in a large cohort of saccular aneurysms. 3D-AWE mapping is a new tool that may improve the identification of symptomatic aneurysms.
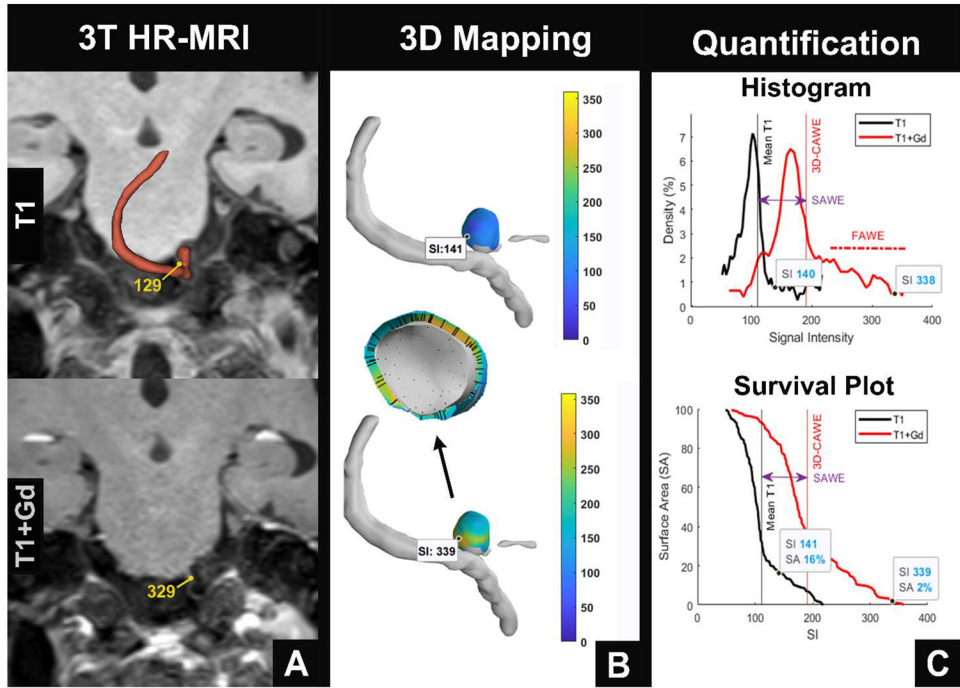
Figure 1. 3D-AWE map of a PICA aneurysm.

(A) Aneurysm segmentations are manually created with 3T HR-MRI, using T1 (top) and T1+Gd (bottom) images. (B) 3D-AWE mapping is generated from orthogonal probes that are automatically extended from the lumen into the aneurysm wall (center). Note that the manual signal intensity (SI) values identified in T1 and T1+Gd images are similar to those obtained through 3D-AWE mapping (T1: 129 vs. 141 and T1+Gd: 329 vs. 339). (C) Quantification of AWE can be visualized through histograms (top) that show the distribution of SI throughout the aneurysm on T1 (black) and T1+Gd (red) images and survival plots (bottom) that identify the surface area of enhancement above different thresholds of SI. Mean SI increases from T1 to T1+Gd imaging with a right shift of the histogram (top). This is defined as SAWE (purple double arrow). There is significant positive skew of the histogram, which is defined as FAWE (top). The survival plot (bottom) shows that on the T1 image, 16% of the aneurysm surface has an SI greater than 141. On the T1+Gd image, only 2% of the aneurysm surface has an SI greater than 339. FAWE is highly concentrated in this area, suggesting that it may be prone to rupture (B, bottom).

PICA = posterior inferior cerebellar artery, AWE = aneurysm wall enhancement, T1+Gd = T1 post contrast gadolinium, SAWE = specific aneurysm wall enhancement, FAWE = focal aneurysm wall enhancement
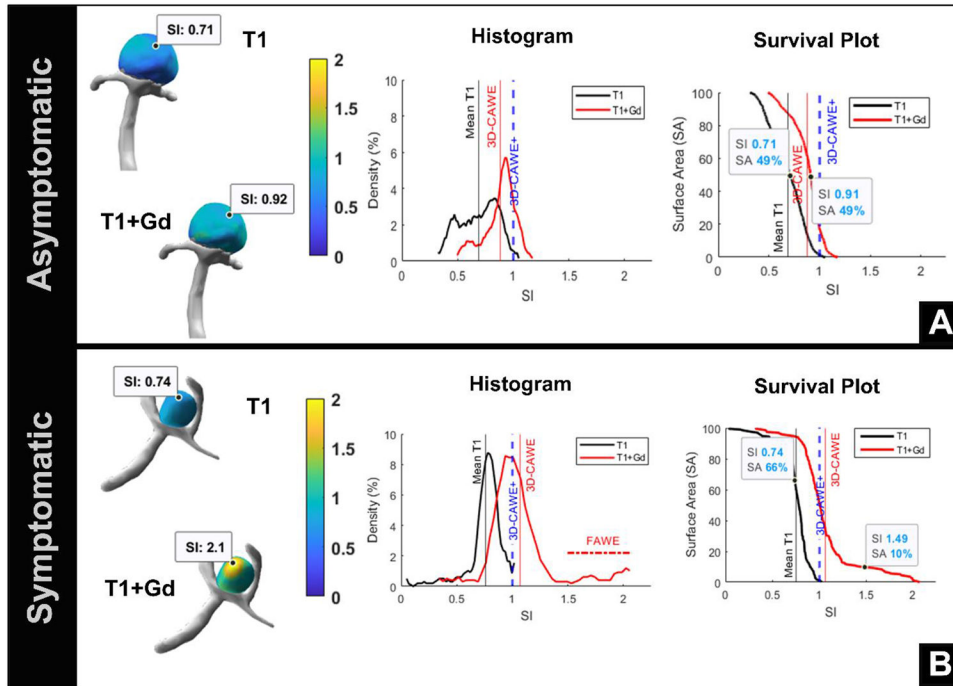
Figure 2. 3D AWE maps of asymptomatic vs symptomatic aneurysms.

(A) An asymptomatic 11-mm basilar tip aneurysm (top) shows a uniform distribution of AWE on the histogram (center) and barely uptakes Gd. This aneurysm is 3D-CAWE– (3D-CAWE < 1). (B) Conversely, a symptomatic 3.5-mm ACOM aneurysm (bottom) is 3D-CAWE+ and has a significant positive skew (FAWE) on the histogram (center). The survival plot (right) shows that approximately 10% of the aneurysm has FAWE. Although this aneurysm is small, it is symptomatic and has a large area of FAWE.

AWE = aneurysm wall enhancement, Gd = gadolinium, 3D-CAWE = 3D circumferential aneurysm wall enhancement, FAWE = focal aneurysm wall enhancement
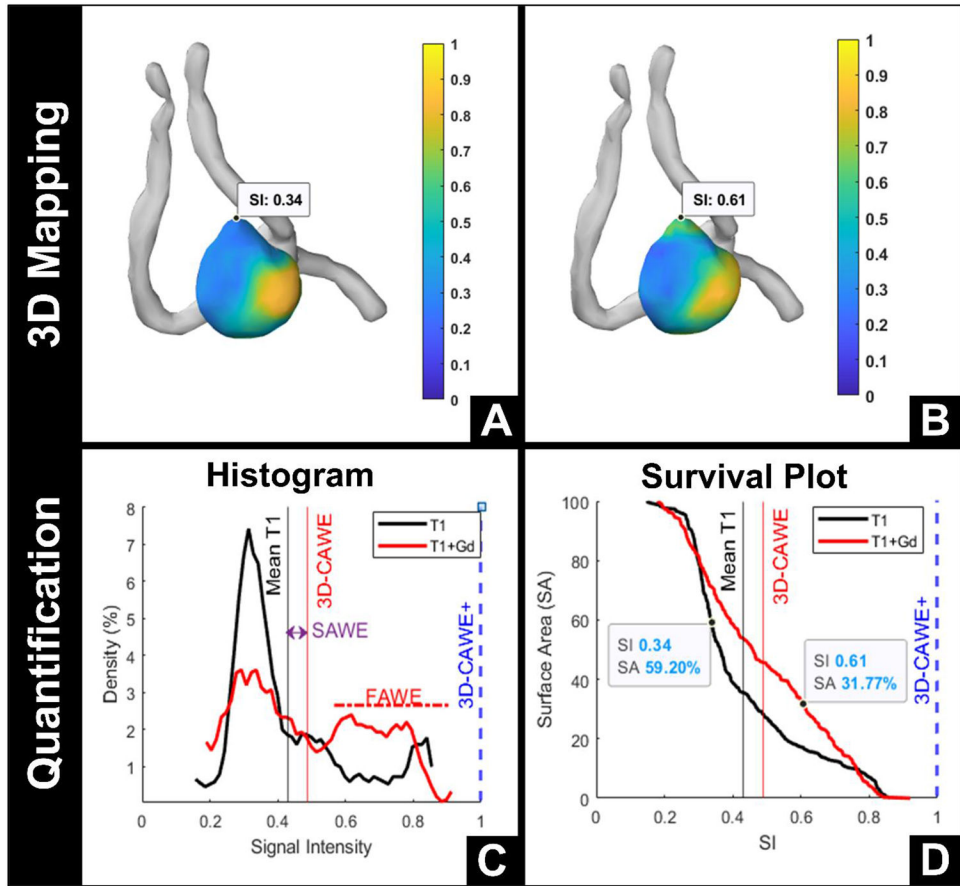
Figure 3. 3D AWE map of an ACOM aneurysm with a bleb.

A 4.6-mm ACOM aneurysm with a bleb that has increased Gd uptake, from T1 (A) to T1+Gd (B) images. The Gd uptake of the bleb is 172% higher than the rest of the aneurysm. The histogram (C) shows a broad distribution of signal intensity (SI) along the entire aneurysm, while the survival plot (D) demonstrates that the percentage of the aneurysm that enhances more than the bleb decreases from T1 (59%) to T1+Gd (32%). This indicates that the bleb picks up more Gd than the rest of the aneurysm.

ACOM = anterior communicating artery, Gd = gadolinium, 3D-CAWE = 3D circumferential aneurysm wall enhancement

Table.

Logistic analysis of predictors of symptomatic status.

Univariate Analysis								
Variable	OR	95% CI	*p*	Cutoff	SP	SN	AUC	NPV
Female	2.14	0.53–14.4	0.3	0.50	0.19	0.90	0.546	0.875
HTN	0.68	0.25–1.88	0.4	0.50	0.64	0.45	0.547	0.810
Family Hx IA	1.05	0.15–4.80	>0.9	0.50	0.63	0.40	0.515	0.793
Smoking	1.90	0.68–5.24	0.2	0.50	0.90	0.10	0.502	0.786
High Risk Location	1.14	0.40–3.10	0.8	0.50	0.63	0.40	0.515	0.793
Irregular	2.66	0.97–7.47	0.058	0.50	0.69	0.55	0.617	0.847
Age	0.94	0.89–0.99	**0.015**	55.5	0.88	0.45	0.328	1.00
Size	1.53	1.23–1.98	**<0.001**	6.2	0.71	0.85	0.790	0.945
SR	1.96	1.38–2.94	**<0.001**	2.28	0.56	0.85	0.756	0.932
AR	2.09	1.25–3.80	**0.008**	1.94	0.86	0.55	0.750	0.875
3D-CAWE [*†]	1.34	1.10–1.67	**0.005**	1.02	0.81	0.65	0.731	0.894
SAWE [*]	1.25	1.00–1.18	**0.047**	0.31	0.74	0.60	0.637	0.871
Skew [*]	1.08	1.00–1.18	**0.049**	0.20	0.66	0.60	0.629	0.857
3D-CAWE+ [†]	7.18	2.51–22.3	**<0.001**	0.50	0.80	0.65	0.722	0.892
Multivariate Model								
Covariates	OR	95% CI	*p*	Cutoff	SP	SN	AUC	NPV
Size	1.49	1.18–2.01	**0.003**	6.2	0.71	0.85	0.790	0.945
3D-CAWE+	4.92	1.22–21.0	**0.026**	0.50	0.80	0.65	0.722	0.892
Age	0.89	0.81–0.96	**0.007**	55.5	0.88	0.45	0.328	1.00
Skew [*]	1.15	1.01–1.34	**0.049**	0.20	0.66	0.60	0.629	0.857
Female	6.05	0.78–123	0.14	0.50	0.19	0.90	0.546	0.875
Model	N/A				0.80	0.90	0.914	0.967

[*] Indicates OR calculated for a 0.1 unit increase, rather than 1.

[†] 3D-CAWE is continuous, while 3D-CAWE+ is the dichotomized classification of aneurysms more enhancing than the corpus callosum (3D-CAWE ≥ 1)

HTN = hypertension, Hx = history, IA = intracranial aneurysm, CAWE = circumferential aneurysm wall enhancement, SAWE = specific aneurysm wall enhancement, OR = odds ratio, CI = confidence interval, SP = specificity, SN = sensitivity, AUC = area under curve, NPV = negative predictive value